Received: 28 August 2023 | Revised: 16 November 2023 | Accepted: 30 November 2023

DOI: 10.1002/hbm.26567

RESEARCH ARTICLE

WILEY

Left ventricular hypertrophy as a risk factor for accelerated brain aging: Results from the Study of Health in Pomerania

Stefan Frenzel[1] | Robin Bülow[2] | Marcus Dörr[3,4] | Stephan B. Felix[3,4] | Nele Friedrich[4,5] | Henry Völzke[4,6] | Katharina Wittfeld[1,7] | Hans J. Grabe[1,7] | Martin Bahls[3,4]

[1]Department of Psychiatry and Psychotherapy, University Medicine Greifswald, Greifswald, Mecklenburg-Western Pomerania, Germany

[2]Institute of Diagnostic Radiology and Neuroradiology, University Medicine Greifswald, Greifswald, Mecklenburg-Western Pomerania, Germany

[3]Department of Internal Medicine B, University Medicine Greifswald, Greifswald, Mecklenburg-Western Pomerania, Germany

[4]German Centre for Cardiovascular Research (DZHK), Partner Site Greifswald, Greifswald, Mecklenburg-Western Pomerania, Germany

[5]Institute of Clinical Chemistry and Laboratory Medicine, University Medicine Greifswald, Greifswald, Mecklenburg-Western Pomerania, Germany

[6]Institute for Community Medicine, University Medicine Greifswald, Greifswald, Mecklenburg-Western Pomerania, Germany

[7]German Center for Neurodegenerative Disease (DZNE), Partner Site Rostock/Greifswald, Greifswald, Mecklenburg-Western Pomerania, Germany

Correspondence
Stefan Frenzel, Department of Psychiatry and Psychotherapy, University Medicine Greifswald, Ellernholzstraße 1-2, Greifswald 17475, Mecklenburg-Western Pomerania, Germany.
Email: stefan.frenzel@uni-greifswald.de

Funding information
Bundesministerium für Bildung und Forschung, Grant/Award Numbers: 01ZZ0701, 01ZZ96030; National Institue of Health, Grant/Award Number: AG059421

Abstract

Previous studies provided evidence for the importance of cardiac structure abnormalities, in particular greater left ventricular (LV) mass, for brain aging, but longitudinal studies are lacking to date. We included 926 individuals (median age 48 years; 53% women) from the TREND cohort of the Study of Health in Pomerania (SHIP) without reduced ejection fraction or a history of myocardial infarction. LV mass index (LVMI) was determined by echocardiography at baseline. Brain morphometric measurements were derived from magnetic resonance images at baseline and 7-year follow-up. Direct effects of baseline LVMI on brain morphometry at follow-up were estimated using linear regression models with adjustment for baseline brain morphometry. At baseline, median LVMI was 40 g/m$^{2.7}$ and 241 individuals (26%) met the criterion of LV hypertrophy. After correction for multiple testing, baseline LVMI was directly associated with reduced global cortical thickness and increased cortical brain age at follow-up independent from hypertension and blood pressure. Exposure-outcome relations were nonlinear and significantly stronger in the upper half of the exposure distribution. Specifically, an increase in baseline LVMI from the 50% quantile to the 95% quantile was associated additional 2.7 years (95% confidence interval = [1.5 years, 3.8 years]) of cortical brain age at follow-up. Additional regional analyses yielded bilateral effects on multiple frontal cortical regions. Our findings highlight the role of cardiac structure in brain aging. LVMI constitutes an easily measurable marker that might help to identify persons at risk for cognitive impairment and dementia.

KEYWORDS
brain aging, brain imaging, epidemiology, left ventricular hypertrophy

Abbreviations: ATC, anatomical therapeutic chemical; BIANCA, Brain Intensity AbNormality Classification Algorithm; CI, confidence interval; *E*/*A*, ratio of early and late wave ventricular filling velocities in diastole; *E*/*e*′, ratio of early ventricular inflow velocity and early mitral annular velocity in diastole; FLAIR, fluid-attenuated inversion recovery; IVSD, interventricular septal thickness; LAI, left atrial size index; LV, left ventricle; LVD, LV end-diastolic diameter; LVH, left ventricular hypertrophy; LVM, left ventricular mass; LVMI, left ventricular mass index; MRI, magnetic resonance imaging; PWD, posterior wall thickness; SHIP, Study of Health in Pomerania; WMH, white matter hyperintensities.

1 | BACKGROUND

During aging, the heart changes in cellular structure which include death of cardiomyocytes, compensatory hypertrophy of remaining cardiomyocytes, and interstitial fibrosis, which may lead to thickening of the walls of the left ventricle (LV) and, eventually, LV hypertrophy (LVH) (Dai et al., 2012; Lakatta & Levy, 2003). These structural changes decrease the elasticity of the ventricular walls, thereby impairing myocardial relaxation and filling during diastole (Lorell & Carabello, 2000). While these changes primarily happen as an adaptation to mechanical stress like chronic pressure overload due to arterial hypertension (Devereux et al., 1993; Ruwhof & van der Laarse, 2000), they have also been observed in the absence of cardiovascular risk factors. Hence, LV thickening is believed to be part of an "intrinsic" cardiac aging process that involves a plethora of molecular mechanisms and is tightly linked to pathological changes in the vascular system, in particular arterial stiffening (Strait & Lakatta, 2012). Not only do these structural and functional changes increase the risk of atrial fibrillation and heart failure, but they also adversely affect the brain via alterations in cerebral hemodynamics and have been associated with an increased risk of cerebral stroke and dementia (Bluemke et al., 2008; de Bruijn et al., 2015; Moazzami et al., 2018; Wolters et al., 2017).

LV mass is a subclinical marker of LVH that can be determined non-invasively via echocardiography or cardiac magnetic resonance imaging (MRI). While LVH is characterized by changes in several structural measurements of the heart, for example, increases in posterior wall thickness, LV mass (LVM) is a well-established surrogate. Several studies found a higher LVM was associated with worse cognitive function (Georgakis et al., 2017; Restrepo et al., 2018), reduced grey matter volume (Frenzel et al., 2021; Haring et al., 2017), and markers of cerebral small vessel disease (Johansen et al., 2018; Nakanishi et al., 2017; Papadopoulos et al., 2020). The few longitudinal studies provided evidence that LVM is directly related to cognitive decline in old age independent of other cardiovascular risk factors and comorbidities (Kähönen-Väre et al., 2004; Mahinrad et al., 2017; Scuteri et al., 2009; van der Veen et al., 2015). However, studies of the underlying brain structural changes are still scarce. One exception is the study by van der Veen et al. (2015), who investigated changes in brain structure as a function of hypertensive target organ damage (defined by LVH, impaired renal function, and albuminuria) after a follow-up time of about 3.9 years. Having at least two hypertensive target organ damages was associated with global brain atrophy, but not with increased white matter hyperintensities (WMH) burden, in 663 patients with manifest coronary artery disease, cerebrovascular disease, peripheral arterial disease, or an abdominal aortic aneurysm. However, direct associations with LVM were not investigated.

In a previous study from this group, cross-sectional associations between LVM and brain morphometry were analysed based on baseline data from the TREND cohort of the population-based Study of Health in Pomerania (SHIP) (Frenzel et al., 2021). After completion of follow-up examinations, the aim of this study was to investigate longitudinal associations of LVM with brain morphometric changes in individuals without reduced LV ejection fraction or a history of myocardial infarction during the 7-year follow-up period. Total brain volume, subcortical grey matter volume, white matter volume, WMH volume, and global cortical thickness were the primary outcomes of this study. We also considered age scores (effective ages) of the cortex, subcortical structures, and the whole brain to represent structural brain changes during the follow-up period to ease with the interpretation of our results (Hertel et al., 2018; Spiegelhalter, 2016). As previous studies provided evidence for the importance of diastolic function with regard to brain aging (Cermakova et al., 2017; Lee et al., 2020; Shimizu et al., 2014), we additionally investigated whether associations with LVM can be explained by alterations in diastolic filling or left atrial size.

2 | METHODS

2.1 | Study sample

The SHIP is a prospective population-based cohort study of adults from West Pomerania, a north-eastern region in Germany with approximately 220,000 inhabitants (Völzke et al., 2022). The data used in our analyses were derived from SHIP-TREND, a cohort initiated 10 years after the initial cohort SHIP-START in the same geographical region. In brief, from the total population of West Pomerania a two-stage stratified cluster sample of 8016 adults between the ages of 20–79 years was drawn. A total of 4420 individuals agreed to participate in the study and took part in the baseline examinations between 2008 and 2012 (SHIP-TREND-0), and 2431 participants (55%) took part in the first follow-up examinations conducted about 7 years later between 2016 and 2019 (SHIP-TREND-1) (Hosten et al., 2022; Völzke et al., 2022). All participants gave written informed consent. The study was approved by the ethics committee of the University Medicine Greifswald and complied with the declaration of Helsinki.

A total of 987 participants without history of myocardial infarction, stroke, or kidney disease received an echocardiography at baseline and brain MRI at baseline and follow-up (see Figure 1). Participants with LV ejection fraction <40% ($n = 8$), time interval between echocardiography and brain MRI being larger than 1 year ($n = 7$), and major structural abnormalities of the brain (e.g., tumors and large cysts), hemorrhages, ischemias, or aneurysms according to radiological findings ($n = 46$) were excluded. The final study sample comprised 926 individuals. Details on data collection are provided by the sections below as well as Supplementary Text 1.

2.2 | Echocardiography

Two-dimensional, M-Mode, and Doppler echocardiography were performed using the Vivid-I system (GE Medical Systems, Waukesha, USA) as described in detail elsewhere (Völzke et al., 2010). Measurements of the LV end-diastolic diameter (LVD, in cm), interventricular septal thickness (IVSD, in cm), as well as posterior wall thickness (PWD, in cm) were performed according to the guidelines of the

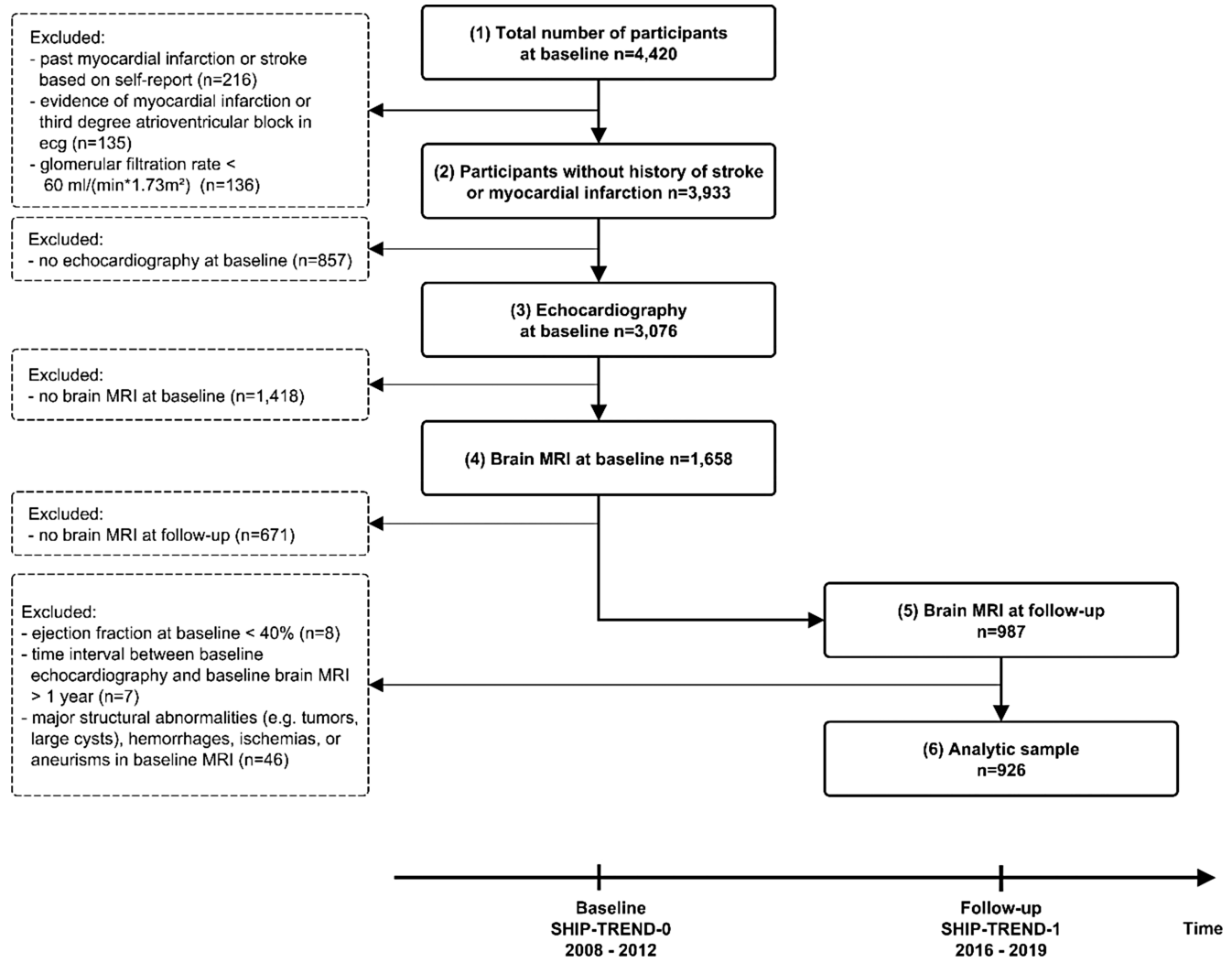

FIGURE 1 Flowchart showing the selection of the study sample. The study sample is based on the TREND cohort of the population-based Study of Health in Pomerania (SHIP). Echocardiography and brain magnetic resonance imaging were performed during the baseline examinations between 2008 and 2012 (SHIP-TREND-0). Follow-up examinations of similar extend were conducted about 7 years later between 2016 and 2019 (SHIP-TREND-1).

American Society of Echocardiography (Lang et al., 2015; Schiller et al., 1989). Left ventricular mass (LVM, in g) was determined according to the formula $LVM = 0.8*1.04*((LVD + IVSD + PWD)^3\text{-}LVD^3)) + 0.6$ as described by Devereux et al. (1986). LVM was indexed to body height to the allometric power of 2.7 ($LVMI = LVM/HEIGHT^{2.7}$) (Cuspidi et al., 2009). Left atrial size index (LAI, in cm/m^2) was defined as the size of the left atrium indexed to body surface area (calculated using the Du Bois formula). Ratio of early and late wave ventricular filling velocities (*E*/*A*), as well as ratio of early ventricular inflow velocity and early mitral annular velocity in diastole (*E*/*e*′) were determined using Doppler echocardiography.

2.3 | Brain morphometry

T1-weighted and T2-weighted fluid-attenuated inversion recovery (FLAIR) scans of the brain were obtained using a 1.5 T Siemens Magnetom Avanto scanner (Siemens Healthineers, Erlangen, Germany) (Hosten et al., 2022). Morphometric measurements of total brain volume, global cortical thickness, subcortical grey matter volume, and white matter volume were derived from T1-weighted images using the longitudinal stream in the image-processing pipeline FreeSurfer version 7.2 which is documented and freely available for download online (Fischl, 2012; Reuter et al., 2012). Cortical thickness but not cortical volume or surface area was considered due to the weaker association with body height and sex, thereby minimizing the nuisance variation shared with structural cardiac measurements. Partly because of that, cortical thickness is generally preferred when deriving markers of neurodegenerative diseases such as Alzheimer's disease (Frenzel et al., 2020; Schwarz et al., 2016). In addition, age-related changes in cortical volume have been found to be primarily related to changes in cortical thickness, not surface area (Storsve et al., 2014).

The processing also includes a parcellation of the cerebral cortex into 34 regions per hemisphere based on the Desikan–Killiany atlas, which has been successfully applied in a wide range of imaging studies

in the past. The underlying method has been shown to give anatomically valid and reliable results (Desikan et al., 2006). FreeSurfer also gives an estimate of the intracranial volume of the head, which can be used to account for some of the variability of the morphometric measurements between the study participants.

WMH volume was determined from FLAIR images based on the Brain Intensity AbNormality Classification Algorithm (BIANCA) (Griffanti et al., 2016) and values were log2 transformed to account for their right-skewed distribution.

2.4 | Brain age scores

In addition to the morphometric measurements described above, age scores were used to represent age-related structural brain changes in better interpretable manner (Hertel et al., 2018; Spiegelhalter, 2016). Brain age (BA) can be considered a hidden biological trait representing the result of the gradual accumulation of brain changes caused by complex psychosocial and biological processes that happen during aging (Cole et al., 2018; Hertel et al., 2018). These processes eventually lead to structural brain changes (e.g., decline in cortical thickness) that can be detected by neuroimaging. Under the assumption of BA being the mediator of the effects of chronological age (A) on some brain parameter X (i.e., the brain does not carry any clock in it and the causal structure can be represented by the directed graph A- > BA- > X), information on the unobservable BA can be derived by a two-step procedure. First, A is regressed on X and the predicted ages (brain age scores) are calculated. Second, the brain age scores are regressed on age and the residuals are calculated. It can be shown that the so-derived residuals contain information on the hidden trait BA (Hertel et al., 2018). Here, we follow the common epidemiological practice to construct these residuals implicitly by adjusting for age in all association analyses rather than explicitly calculating them.

Cortical BA was derived from the thicknesses of 64 cortical regions defined by the Desikan-Killiany atlas. Subcortical BA was defined based on volumes of deep grey matter nuclei (thalamus, caudate, putamen, pallidum, hippocampus, amygdala, ventral diencephalon, and nucleus accumbens) and ventricle volumes (lateral ventricle, inferior lateral ventricle, third ventricle, and fourth ventricle) of both hemispheres (22 brain parameters). (Global) BA was defined based on the union of parameters used for calculating cortical and subcortical BA (86 brain parameters). Estimation of brain age models was performed using baseline data by linear regressions of chronological age on the corresponding set of brain parameters for each sex separately. As the sample size is at least 10 times the number of brain parameters, we can expect the so-derived BA models to be reliable and to perform reasonably well on independent data (Harrell, 2015). BA scores at baseline and follow-up were then predicted based on the so-derived regression models. The well-known age-specific estimation bias, that is, BA overestimating chronological age in young individuals and underestimation in the old, was corrected by forcing the slope to one and intercept to zero (see Figure S1) (Beheshti et al., 2019; de Lange & Cole, 2020).

2.5 | Statistical analyses

The primary outcomes of our study are given in Table 1. Direct effects of LVMI on changes in the outcomes were analysed by weighted

TABLE 1 Primary outcomes of the study. Morphometric measurements were derived from T1-weighted and T2-FLAIR brain scans. In addition, age scores were considered in order to measure the age-related atrophy of the cerebral cortex (cortical brain age), subcortical structures (subcortical brain age), and both together (brain age) in a better interpretable manner.

Outcome	Unit	Comments
Morphometric measures		
Total brain volume	mL	Without cerebellum, brain stem, ventricles, or CSF; volume- and surface-based processing of T1-weighted images with FreeSurfer 7.2 (Fischl, 2012; Reuter et al., 2012)
Subcortical grey matter volume	mL	Total volume of deep grey matter nuclei (thalamus, caudate, putamen, pallidum, hippocampus, amygdala, accumbens area, ventral diencephalon); volume-based processing of T1-weighted images with FreeSurfer 7.2 (Fischl, 2012; Reuter et al., 2012)
White matter volume	mL	Without cerebellar white matter or brainstem, surface- and volume-based processing of T1-weighted images with FreeSurfer 7.2 (Fischl, 2012; Reuter et al., 2012)
White matter hyperintensities volume	mm^3	Derived from T1-weighted and T2-FLAIR images with BIANCA (Griffanti et al., 2016)
Global cortical thickness	mm	Average thickness of the cerebral cortex; surface-based processing of T1-weighted images with FreeSurfer 7.2 (Fischl, 2012; Reuter et al., 2012)
Age scores		
Cortical brain age	years	Based on thicknesses of cortical regions according to the Desikan-Killiany atlas (Desikan et al., 2006) (64 regions) from surface-based processing with FreeSurfer 7.2
Subcortical brain age	years	Based on individual volumes of deep gay matter nuclei and ventricles (22 regions) from volume-based processing with FreeSurfer 7.2
Brain age	years	Based on union of features used for the calculation of cortical and subcortical brain age

linear regressions of follow-up values of the outcomes (not changes from baseline) on baseline LVMI with adjustment for baseline values of the outcomes (see Figure 2) (Tennant et al., 2022; Twisk, 2013; Vanderweele, 2015). Analyses were adjusted for baseline values of sociodemographic variables (age, sex, number of years of education, employment status, equalized disposable income, and marital status), anthropometric variables (body height, body weight, intracranial volume), lifestyle factors (smoking status, alcohol consumption), and follow-up time (model 1). In addition, we adjusted for cardiovascular risk factors (diabetes, hypertension, waist-to-height ratio, cholesterol ratio, intake of lipid-lowering drugs, diastolic blood pressure, pulse pressure, intake of antihypertensive drugs; model 2). Mediation by diastolic function was investigated by additionally including the ratio of early and late mitral inflow velocities in diastole (E/A), the ratio of early mitral inflow velocity and early mitral annular velocity in diastole (E/e'), and the left atrial size index, with the latter being a surrogate marker for advanced diastolic dysfunction (Thomas et al., 2019) (model 3). Under the assumptions of no exposure–mediator interactions, the presence of mediation was assessed by comparing the so-derived effect estimates with those from model 2 (Vanderweele, 2015). To avoid lowering the sample size because of missing values in the control variables, multivariate imputation was performed. Predictive mean matching was used for continuous variables and multinomial logistic regressions for categorical ones (van Buuren & Groothuis-Oudshoorn, 2011).

Continuous control variables were z-transformed and the relationships with outcomes were modeled in a flexible way by restricted cubic splines with three knots located at the 10%, 50%, and 90% quartiles (Harrell, 2015). This allows for a wide range of possible relationships (e.g., linear and U-shaped) while spending only two degrees of freedom for each variable. Interactions were pre-specified based on background knowledge. We followed the general rule to particularly include interactions between control variables that have large coefficients when interactions are not considered. In all three models we therefore included the interaction between age and sex, which are strongly and independently associated with brain and cardiac structure. Since cholesterol ratio and blood pressure are affected by commonly prescribed drugs, we additionally included their interaction with intake of lipid-lowering and antihypertensive medication, respectively, in models 2 and 3. The ratios of sample size (n) to numbers of degrees of freedom (df) are sufficiently large to avoid overfitting any of the three models (Harrel considers $n/df > 15$ as good average requirement which is fulfilled in our study [Harrell, 2015]).

Our study sample differed from the participants of the baseline examination. Echocardiographic assessment of cardiac structure was not possible in a substantial portion of them due to poor image quality (e.g., due to obesity). Sociodemographic and health-related factors may have influenced the ability and willingness to participate in the two additional MRI examinations. Inverse probability weights were used to account for these biases and to increase the generalizability of the results (Weuve et al., 2012). First, for participants without history of myocardial infarction or stroke at baseline, availability of echocardiography and brain MRI at baseline was modeled by logistic regressions on baseline values of sociodemographic variables, smoking status, alcohol consumption, diabetes, hypertension, and waist-to-height ratio (steps 2–4 in Figure 1). Second, for participants who

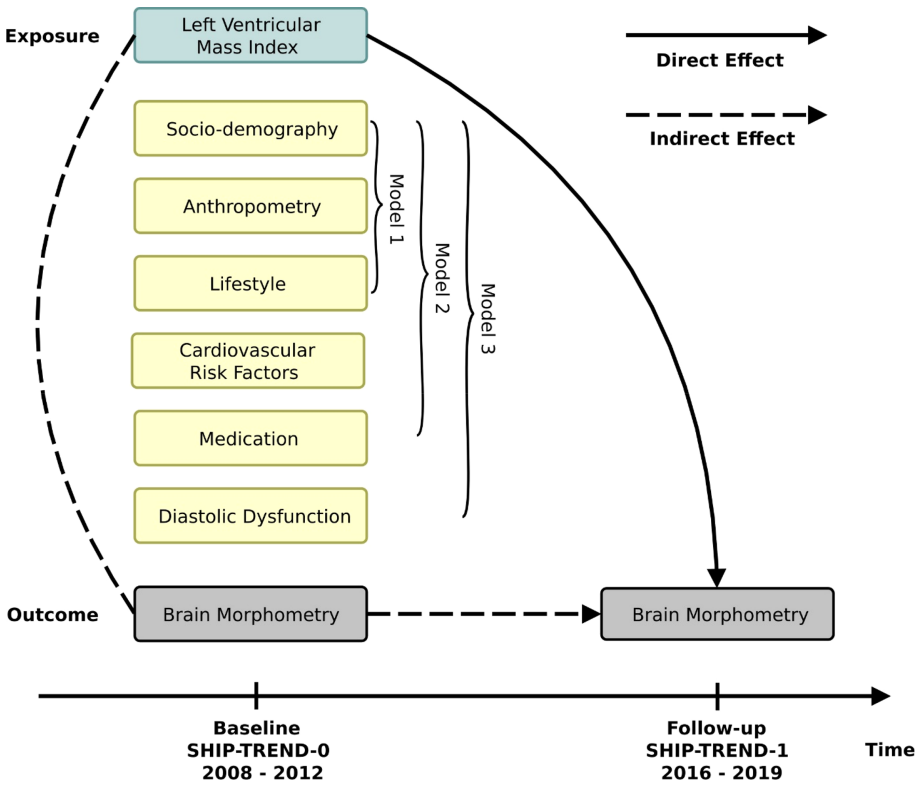

FIGURE 2 Direct effects of baseline LVMI on changes in brain morphometry. Weighted linear regressions of follow-up values of the outcomes (brain volume, subcortical grey matter volume, white matter volume, white matter hyperintensities volume, global cortical thickness, cortical brain age, subcortical brain age, and brain age) on baseline LVMI with adjustment for baseline values of the outcomes were performed. Analyses were additionally adjusted for baseline values of sociodemographic variables, anthropometric variables, lifestyle factors, and follow-up time (model 1). In addition, we adjusted for cardiovascular risk factors and intake of antihypertensive and lipid-lowering drugs (model 2). Mediation by diastolic function was investigated by including E/e' ratio, E/A ratio, and left atrial size index (model 3). E/A—ratio of early and late mitral inflow velocities in diastole. E/e'—ratio of early mitral inflow velocity and early mitral annular velocity in diastole. LVMI, left ventricular mass index.

underwent echocardiography and brain MRI at baseline, the availability of brain MRI at the follow-up was modeled in the same way (steps 4–5 in Figure 1). Using the chain rule, the final weights were calculated as the product of the reciprocal values of these probabilities. Weights above the 99% quantile were trimmed down.

To avoid spurious associations due to a small number of highly influential cases, values of Cook's distance and absolute values of DFBETA were calculated. As two degrees of freedom were used for modeling of the exposure, the maximum absolute value of both was considered. Cases exceeding recommended thresholds were excluded from the analyses (Rawlings et al., 1998). Effect sizes were assessed with partial Cohen's f^2 which equals the proportion of variance uniquely accounted for by a particular variable beyond all other variables. In addition, point estimates of effects were derived from changes in outcomes when baseline LVMI is increased from the 50% to the 95% quantile while holding continuous control variables at their median values and categorical ones at their reference category (Harrell, 2015). We used the Benjamini–Hochberg method with false discovery rate ≤ 5% to account for multiple testing of eight outcomes. All statistical analyses were performed with R version 4.05 and the *rms* package (Harrell, 2015). Imputations were performed with the package *mice* (van Buuren & Groothuis-Oudshoorn, 2011) and figures were created with *ggplot* (Valero-Mora, 2010).

3 | RESULTS

3.1 | Sample characteristics

A total of 926 individuals from 21 to 80 years of age, with a median age of 48 years, were included in the study sample with 53% ($n = 486$) being women. Sample characteristics are shown in Table 2. Missing values in covariates were replaced with estimates based on multivariate imputation (missing rates <9%). The median time interval between brain MRIs at baseline and follow-up was 7.3 years (first quartile 7.1 years, third quartile 7.5 years, min. 5 years, max. 10.2 years). Hypertension and diabetes mellitus were present in 35% ($n = 323$) and 5% ($n = 44$), respectively, of the study population. A total of 43% and 38% were never smokers and former smokers, respectively. For participants for whom echocardiographic measurements were available at baseline, median value of LVMI was 40.6 g/$m^{2.7}$ (men: 43.8 g/$m^{2.7}$; women: 37.8 g/$m^{2.7}$) and the 95% quantile was 63.1 g/$m^{2.7}$ (men: 65.9 g/$m^{2.7}$; women: 58.8 g/$m^{2.7}$). Summary statistics of brain morphometry measures and age scores (primary outcomes) are shown in Table 3. Intra-individual variability was low with intra-class correlations between baseline and follow-up values ranging from 0.90 for WMH volume (log-transformed) to 0.99 for total brain volume.

There was evidence for selection bias with respect to age, waist-to-height ratio, smoking, and number of years of education. Age was by far the strongest predictor of availability of echocardiographic measurements and brain MRI at baseline (steps 2–4 in Figure 1, $\chi_4^2 = 69.7$, $p < .0001$), followed by numbers of years of education and

TABLE 2 Baseline characteristics.

	Participants without history of stroke or myocardial infarction ($N = 3932$)	Study sample ($N = 926$)
Sociodemographic		
Age, years	51.1 (41.0, 61.2)	48.1 (40, 57.7)
Women, %	52.7	52.5
Body height, cm	170 (163, 177)	171 (164, 178)
Body weight, kg	79.1 (68.3, 91.45)	77.3 (68.03, 87.7)
Number of years of education, years	11 (11, 13)	13 (11, 15)
Marital status		
Single, living alone	11.7	9.9
Living together with partner	77.9	82.5
Divorced, living alone	6.3	5.5
Widowed, living alone	4.1	2.1
Employment		
Unemployed	9.7	6.4
Student	2.6	3.8
Employed	59.6	72
Pensioner	28.1	17.8
Equalized disposable income, €	1184 (895, 1775)	1450 (1096, 1803)
Cardiovascular risk factors		
Smoking status		
Never	36.4	42.8
Former	35.4	37.7
Current	28.2	19.5
Alcohol consumption, g/d	3.6 (0.7, 10.8)	4.6 (1.3, 11.1)
Waist-to-height ratio, %	0.52 (0.47, 0.58)	0.5 (0.46, 0.55)
Diabetes mellitus, %	9.8	4.8
Hypertension, %	44.5	34.9
Systolic blood pressure, mmHg	126.5 (114, 139)	123 (112, 135)
Diastolic blood pressure, mmHg	76.5 (70.5, 83.5)	76 (70, 82.5)
Pulse pressure, mmHg	48 (40.5, 57)	46.5 (39.5, 54)
HDL-cholesterol ratio, %	3.79 (3.11, 4.68)	3.71 (3.05, 4.5)
Glomerular filtration rate, mL/(min*1.73 m^2)	104.1 (91.8, 115.2)	106.8 (96.6, 116.0)
Medication		
Intake of antihypertensive drugs, %	34.6	25.3
Intake of lipid-lowering drugs, %	9.3	5.3

(Continues)

TABLE 2 (Continued)

	Participants without history of stroke or myocardial infarction ($N = 3932$)	Study sample ($N = 926$)
Echocardiography		
Left ventricular mass, g	171.5 (137.5, 211.2)	169.8 (137.6, 205.2)
Missing	854	0
Left ventricular mass index, g/m$^{2.7}$	40.6 (33.8, 48.4)	39.6 (33.9, 46.2)
Missing	855	0
Ejection fraction, %	71.6 (65.5, 77.3)	72.4 (66.8, 78.5)
Missing	852	1
E/e', %	594 (498, 713)	588 (496, 694)
Missing	0	0
E/A, %	110 (89, 140)	116 (96, 144)
Missing	0	0
Left atrial size index, cm/m^2	2.02 (1.87, 2.19)	2 (1.86, 2.18)
Missing	0	0

TABLE 3 Brain morphometry measures and age scores in the final study sample ($N = 926$).

	SHIP-TREND-0 (baseline)	SHIP-TREND-1 (follow-up)
Age, years	48.1 (40, 57.7)	55.6 (47.3, 65)
Follow-up time, years	-	7.3 (7.1, 7.5)
Intracranial volume, mL	1582 (1471, 1708)	1582 (1471, 1708)
Morphometric measures		
Brain volume, mL	1013 (942, 1096)	994 (920, 1076)
Subcortical grey matter volume, mL	57.2 (53.9, 61)	55.9 (52.5, 59.7)
White matter volume, mL	485 (444, 528)	477 (434, 523)
White matter hyperintensities volume, mm^3	121 (44, 324)	209.5 (58.25, 797)
Global cortical thickness, mm	2.37 (2.3, 2.44)	2.34 (2.27, 2.4)
Age scores		
Cortical brain age, years	48.4 (36.7, 59.7)	54 (41.5, 66)
Subcortical brain age, years	47.3 (35.4, 61.2)	53.2 (41.4, 69.5)
Brain age, years	47.6 (37.4, 58.9)	53.8 (42.8, 66.5)

Note: Values are given as medians with confidence intervals (25% and 75% quantiles).

waist-to-height ratio, with smaller likelihoods for both very young and very old participants ($R^2 = .14$, AUC = 0.68). The corresponding prediction plots are shown in Figure S2. For those participants for whom echocardiographic measurements and brain MRI at baseline were available, availability of brain MRI at follow-up was most strongly predicted by smoking status (steps 4–5 in Figure 1, $\chi_2{}^2 = 31.4$, $p < .0001$), with smaller likelihoods for current smokers ($R^2 = .12$, AUC = 0.68; see Figure S3). Figure S4 shows the final sample weights, which were used in all subsequent regression analyses. Distribution of weights was reasonable and 10 cases were to be trimmed down to the 99% quantile of 5.3.

3.2 | Associations of baseline LVMI with changes in brain morphometry

The recommended thresholds for Cook's distance and absolute values of DFBETA (e.g., $4/n = 0.004$ and $2/\sqrt{n} = 0.066$) (Rawlings et al., 1998), were too strict, probably due to the use of sample weights, and were relaxed to 0.01 and 0.2, respectively. This resulted in the exclusion of about 3% of cases. Cook's distances and DFBETA values for global cortical thickness (model 1) are shown in Figure S5.

LVMI at baseline was associated with the decreased global cortical thickness ($F_{2,864} = 9.3$, $p_{FDR} = .0008$, $f^2 = 2.2\%$), and increased cortical brain age ($F_{2,853} = 7.2$, $p_{FDR} = .003$, $f^2 = 1.7\%$) at follow-up, but not with total brain volume ($F_{2,859} = 0.9$, $p_{FDR} = .5$, $f^2 = 0.2\%$), subcortical grey matter volume ($F_{2,859} = 0.4$, $p_{FDR} = .7$, $f^2 = 0.1\%$), white matter volume ($F_{2,862} = 0.4$, $p_{FDR} = .7$, $f^2 = 0.1\%$), WMH volume ($F_{2,858} = 3.1$, $p_{FDR} = .1$, $f^2 = 0.7\%$), subcortical brain age ($F_{2,853} = 1.5$, $p_{FDR} = .2$, $f^2 = 0.3\%$), or brain age ($F_{2,855} = 2.6$, $p_{FDR} = .1$, $f^2 = 0.6\%$) (model 1). Associations with global cortical thickness and cortical brain age remained stable against additional adjustments for cardiovascular risk factors (including hypertension and blood pressure) and medication (model 2; see Figure 3). Among cardiovascular risk factors, only diabetes mellitus exhibited effects of similar order of magnitude on global cortical thickness ($f^2 = 1.3\%$), followed by alcohol consumption ($f^2 = 0.9\%$). Pulse pressure and its interaction with antihypertensive medication explained a substantial amount of variance of cortical brain age ($f^2 = 3.3\%$), followed by smoking status ($f^2 = 2.0\%$). Detailed results of the analyses of variance can be found in Tables S1–S8. Results of complete case analyses are provided in Tables S10–S17.

Associations of LVMI were significantly stronger in the upper half of the exposure distribution, above the threshold of about 46 g/m$^{2.7}$. This cutoff is approximately the definition of LVH which corresponds to 44 g/m$^{2.7}$ for women and 48 g/m$^{2.7}$ for men ($n = 241$ [26%] of the total study population) (Lang et al., 2015). Point estimates of effects derived from changes in outcomes when baseline LVMI increased from the 50% quantile to the 95% quantile, a reduction of 0.017 mm (95% CI = [0.025 mm, 0.001 mm]) in global cortical thickness and additional 2.7 years (95% CI = [1.5 years, 3.8 years]) of cortical brain age was found. Importantly, there was little change of the estimates and their standard errors between the models. Point estimates of the direct effects of baseline LVMI on all primary outcomes at follow-up are shown in Table 4.

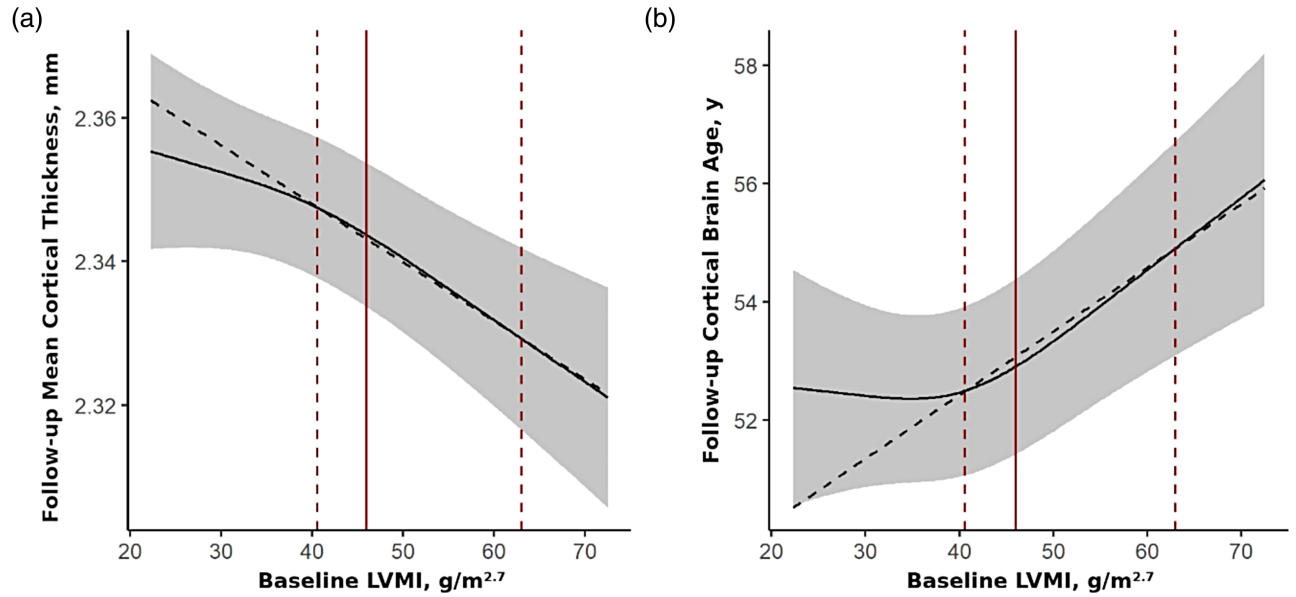

FIGURE 3 Baseline LVMI is associated with global cortical thinning and accelerated cortical aging during the 7-year follow-up period. Direct effects of baseline LVMI on global cortical thickness (a; $F_{2,839} = 9.2$, $p_{FDR} = .0004$, $f^2 = 2.2\%$), and cortical brain age (b; $F_{2,836} = 10.8$, $p_{FDR} = .0002$, $f^2 = 2.6\%$) at follow-up are shown (continuous covariates held constant at their median values and categorical ones at their reference categories). Effects adjusted for baseline values of sociodemographic factors, anthropometric variables, lifestyle factors, cardiovascular risk factors (incl. hypertension and blood pressure) and medication, follow-up time, and baseline value of the outcome (model 2). Grey areas represent the 95% confidence intervals. Point estimates of effects were derived from changes in outcomes when baseline LVMI is increased from the 50% to the 95% quartile (red dashed lines). Red solid lines correspond to the threshold of LV hypertrophy of about 46 g/m$^{2.7}$ (women: 44 g/m$^{2.7}$, men: 48 g/m$^{2.7}$). LV, left ventricular; LVMI, left ventricular mass index.

In sensitivity analyses, the observed associations were robust against changes in the type of indexation of LVM (e.g., by body surface area instead of heigth$^{2.7}$). Additional exclusion of participants with mildly reduced LV ejection fraction of 40%–49% ($n = 12$) did not lead to significant changes in results.

3.3 | The potential mediating role of diastolic dysfunction

In regression models adjusted for markers of diastolic dysfunction (model 3), E/e' exhibited independent direct effects on WMH volume ($F_{2,834} = 5.6$, $p_{FDR} = .02$, $f^2 = 1.4$), and subcortical brain age ($F_{2,829} = 7.3$, $p_{FDR} = .006$, $f^2 = 1.8$) at follow-up, while left atrial size index was associated with WMH volume at follow-up ($F_{2,834} = 5.3$, $p_{FDR} = .04$, $f^2 = 1.3$). However, LVMI was still significantly and independently associated with global cortical thickness ($F_{2,832} = 8.9$, $p_{FDR} = .0006$, $f^2 = 2.1$) and cortical brain age ($F_{2,830} = 11.1$, $p_{FDR} = .0001$, $f^2 = 2.7$) at follow-up, and point estimates were not significantly different from those based on model 2 (see Table 4).

3.4 | Associations of baseline LVMI with regional cortical thinning

In analyses adjusted for cardiovascular risk factors according to model 2, LVMI exhibited significant negative bilateral effects on the thickness of multiple regions of the frontal cortex (caudal middle frontal cortex, superior frontal gyrus, pars triangularis, and precentral gyrus), postcentral gyrus, fusiform gyrus, supramarginal gyrus, and lateral occipital gyrus at follow-up. In addition, unilateral effects were observed in several other cortical regions. Results for all cortical regions are listed in Table S9 and visualized in Figure S6.

4 | DISCUSSION

The role of cardiovascular risk factors for brain aging is well established. Several longitudinal studies also point to the importance of cardiac structure abnormalities, in particular increased LVM, for cognitive decline and dementia (Kähönen-Väre et al., 2004; Mahinrad et al., 2017; Moazzami et al., 2018; Scuteri et al., 2009; van der Veen et al., 2015). Longitudinal studies of the underlying changes in brain structure are lacking to date. In this study, based on data of 926 individuals without reduced ejection fraction and no history of myocardial infarction or stroke, associations of LVMI with changes in brain morphometry over a follow-up period of about 7 years were investigated. LVMI at baseline was significantly associated with reduced global cortical thickness and increased cortical brain age at follow-up independent from hypertension and blood pressure. Albeit systolic function was preserved in our study population, we may have included subjects with heart failure with preserved ejection fraction. However, our results could not be explained by markers of diastolic function. E/e' and LAI were independently associated with changes in WMH burden

TABLE 4 Point estimates of direct effects of baseline LVMI on primary outcomes at follow-up.

	Model 1		Model 2		Model 3	
	Effect size (95% CI)	*t*	Effect size (95% CI)	*t*	Effect size (95% CI)	*t*
Total brain volume, mL	−1.072 (−2.86, 0.715)	−1.18	−0.436 (−2.724, 1.852)	−0.37	−1.124 (−3.233, 0.985)	−1.05
Global cortical thickness, mm	−0.014 (−0.02, −0.007)	−3.94***	−0.017 (−0.025, −0.009)	−4.04***	−0.017 (−0.026, −0.009)	−3.98***
Subcortical grey matter volume, mL	−0.01 (−0.142, 0.121)	−0.16	0.01 (−0.131, 0.152)	0.14	0.001 (−0.149, 0.152)	0.02
White matter volume, mL	0.614 (−0.88, 2.108)	0.81	0.752 (−0.892, 2.397)	0.9	0.868 (−0.87, 2.605)	0.98
White matter hyperintensities volume, mm^3	0.231 (0.046, 0.417)	2.44*	0.17 (0.002, 0.337)	1.99	0.167 (0.001, 0.334)	1.98
Cortical brain age, years	1.953 (0.84, 3.066)	3.44**	2.661 (1.536, 3.786)	4.64***	2.878 (1.678, 4.078)	4.71***
Subcortical brain age, years	−0.588 (−1.514, 0.338)	−1.25	−0.434 (−1.444, 0.575)	−0.84	−0.755 (−1.812, 0.303)	−1.4
Brain age, years	0.7 (0.067, 1.333)	2.17	0.517 (−0.1, 1.133)	1.64	0.613 (−0.024, 1.249)	1.89

Note: Model 1: sociodemographic factors, anthropometric variables, lifestyle factors (including education, smoking, and alcohol consumption), follow-up time, and baseline value of the outcome. Model 2: model 1 + cardiovascular risk factors (including hypertension and pulse pressure) and medication. Model 3: model 2 + markers of diastolic function.

Abbreviations: CI, confidence interval; LVMI, left ventricular mass index.

*p_{FDR} < .05.**p_{FDR} < .01.***p_{FDR} < .001.

and subcortical brain age, which is in line with previous studies (Cermakova et al., 2017; Lee et al., 2020; Shimizu et al., 2014). LVMI was the strongest predictor of changes in global cortical thickness among all cardiovascular risk factors. Regarding cortical brain age, only pulse pressure exhibited stronger effects than LVMI. No evidence for associations with total brain volume, subcortical grey matter volume, white matter volume, WMH volume, subcortical brain age, or (global) brain age, was found.

Our results are also in agreement with previous studies reporting associations of LVMI with reduced thickness of the cerebral cortex (Frenzel et al., 2021) and brain atrophy in individuals with chronic exposure to high blood pressure (van der Veen et al., 2015). However, we did not find an association with WMH volume reported by several cross-sectional studies (Frenzel et al., 2021; Johansen et al., 2018; Nakanishi et al., 2017; Papadopoulos et al., 2020). This could be due to higher intra-individual variability compared to other outcomes in our study. The latter were derived from the longitudinal stream in the image-processing pipeline FreeSurfer which creates a within-subject template space and image to significantly increase reliability and power (Reuter et al., 2012). In contrast, WMH volumes were estimated independently for baseline and follow-up. van der Veen et al. (2015), who investigated changes of brain structure in relation to hypertensive organ damage in patients with manifest coronary artery disease, cerebrovascular disease, peripheral arterial disease, or an abdominal aortic aneurysm, also did not find an association with changes in WMH volumes. The authors attributed this to selective survival but also point towards the fact, that WMH have a large "non-vascular" component with cardiovascular risk factors explaining only a small portion of its variance (Wardlaw et al., 2014). Additional analyses of single cortical regions yielded bilateral effects on multiple regions of the frontal cortex which may explain the deficits in executive function observed in individuals with LVH (Restrepo et al., 2018). Both functional and structural MRI studies provided evidence that the middle frontal, superior frontal, and precentral gyrus, which were all associated with LVMI in our study, are related to cardiorespiratory fitness, an important marker for cardiovascular health (Reiter et al., 2015). Cross-sectional association of LVM with the thickness of the inferior frontal gyrus has been reported (Frenzel et al., 2021). In addition, the middle frontal and precentral gyrus, both stretching over the watershed area of the anterior and middle cerebral artery, have been found to be particularly vulnerable to ischemia, for which LVH is an important risk factor (Payabvash et al., 2011).

While our results are mostly consistent with those reported in past studies, some studies did not find evidence for an association of LVH with cerebral atrophy. In a study based on data of 627 participants of the Coronary Artery Risk Development in Young Adults (CARDIA) study, LVM in young adulthood was not associated with volumetric markers of brain aging in midlife (Cermakova et al., 2017). There are several potential explanations for this. First, LVM primarily reflects long-term exposure to pressure overload. Hence, LVM may become informative regarding brain aging not until mid-life. Second, cortical thickness and cortical brain age were determined using surface-based image processing in our study, which is different from the outcomes considered in the study performed by Cermakova et al. In addition, larger heterogeneity in the study population (e.g., with respect to ethnicity [Drazner et al., 2005]) may also play a role.

Nonlinear modeling of exposures and control variables is neglected in many epidemiological studies. One strength of our study

is that the relations between the outcome variables and continuous exposure and control variables were modeled in a flexible way by restricted cubic splines. We found the relationships of LVMI with cortical thickness and cortical brain age to be monotonous but significantly stronger in the upper half of the LVMI distribution. This is in line with the notion that increases in LVM may be physiological within a certain range, for example, in response to regular exercise (Markus et al., 2021), and highlights the importance of considering nonlinear relationships.

There are several limitations with regard to our analyses. Our study aimed to investigate the direct effects of LVMI on brain aging. For the estimated effects to have a causal interpretation, several statistical assumptions must be fulfilled, most importantly the absence of unmeasured confounding (Tennant et al., 2022; Vanderweele, 2015). Chronic untreated hypertension could constitute such a confounder, as it has both been implicated in LVH (Bülow et al., 2018; Devereux et al., 1993) and brain aging (Debette et al., 2011), and may not always be detected by a single blood pressure measurement (Kario, 2018). In addition, the associations observed in our study could also be explained by changes in the vascular system, in particular increased aortic stiffness (Strait & Lakatta, 2012). The latter causes transmission of excessive flow pulsatility into the microcirculation of the brain due to reduced impedance mismatch with the carotid arteries. This leads to impaired autoregulation of cerebral perfusion and increases the likelihood of microinfarcts and degeneration of brain tissue (Haidar et al., 2021; Mitchell et al., 2011). On the other hand, increased LV afterload contributes to the pathogenesis of LVH. LVMI can thus be considered an integrative marker reflecting both exposure to risk factors in the past and pathological changes throughout the cardiovascular system, and unmeasured confounding is impossible to rule out based on observational studies such as ours. We would like to point out, however, that we did adjust for a wide range of cardiovascular risk factors (including hypertension and blood pressure at baseline). The effect sizes for global cortical thickness and cortical brain age were moderate to strong, which highlights the importance of LVMI as a risk factor for brain aging. Abnormal pulse formation and conduction in the hypertrophied heart predisposing to arrhythmias and increasing the likelihood of cerebral hypoperfusion constitute potential independent mechanisms behind the associations observed in this study.

In our study, LVM was estimated using the Devereux formula which relies on an approximation of the LV by a prolate ellipsoid with long- to short-axis length of 2:1 (Devereux et al., 1986). Determination by cardiac MRI, on the other hand, is more accurate and has emerged as the gold standard for characterizing cardiac function and structure, and should therefore generally be preferred over echocardiography. Its application is limited, however, by the larger cost and the exclusion of subjects with kidney disease when relying on gadolinium contrast agents. As LVH is highly common in subjects with advanced kidney disease, studies relying on cardiac MRI may underestimate the adverse effects of LVH.

Another limitation of our study is that participants were drawn from the population of Western Pomerania and results may not be generalizable to other populations. In addition, inverse probability weighting based on various sociodemographic and health-related factors (e.g., smoking and income) was used to account for selection bias, but other unmeasured factors influencing the participation of individuals may have biased our analyses.

In summary, our findings highlight the role of cardiac structure in brain aging. LVMI constitutes an easily measurable marker that might help to identify the person at risk for cognitive impairments and dementia. Whether normalization of LVM in addition to blood pressure control reduces these risks remains to be established.

AUTHOR CONTRIBUTIONS

Stefan Frenzel and Martin Bahls designed the study. Stefan Frenzel performed the statistical analysis and wrote the manuscript. Stefan Frenzel and Katharina Wittfeld performed the MRI preprocessing. Robin Bülow, Marcus Dörr, Stephan B. Felix, Nele Friedrich, Henry Völzke, and Hans J. Grabe contributed essentially to the data collection. All authors approved the final manuscript before submission.

ACKNOWLEDGMENTS

The Study of Health in Pomerania (SHIP) is part of the Community Medicine Research Net (CMR) (http://www.medizin.uni-greifswald.de/icm) of the University of Greifswald funded by grants from the German Federal Ministry of Education and Research (BMBF, grants 01ZZ96030 and 01ZZ0701). The MRIs in SHIP were supported by a joint grant from Siemens Healthineers, Erlangen, Germany, and the Federal State of Mecklenburg-Western Pomerania. This study was further supported by the National Institute of Health (NIH) grant RF1 AG059421. Open Access funding enabled and organized by Projekt DEAL.

CONFLICT OF INTEREST STATEMENT

HJG has received travel grants and speakers honoraria from Fresenius Medical Care, Neuraxpharm, Servier, and Janssen Cilag as well as research funding from Fresenius Medical Care. All other authors have nothing to disclose.

DATA AVAILABILITY STATEMENT

Data of the SHIP study can be obtained from the Transferstelle für Daten- und Biomaterialienmanagement (https://transfer.ship-med.uni-greifswald.de/FAIRequest/data-use-intro) upon reasonable request from qualified researchers.

ORCID

Stefan Frenzel https://orcid.org/0000-0001-5087-5970
Robin Bülow https://orcid.org/0000-0003-1884-5784
Marcus Dörr https://orcid.org/0000-0001-7471-475X
Stephan B. Felix https://orcid.org/0000-0002-0744-091X
Nele Friedrich https://orcid.org/0000-0002-1017-7622
Henry Völzke https://orcid.org/0000-0001-7003-399X
Katharina Wittfeld https://orcid.org/0000-0003-4383-5043
Hans J. Grabe https://orcid.org/0000-0003-3684-4208
Martin Bahls https://orcid.org/0000-0002-2016-5852

REFERENCES

Beheshti, I., Nugent, S., Potvin, O., & Duchesne, S. (2019). Bias-adjustment in neuroimaging-based brain age frameworks: A robust scheme. *NeuroImage: Clinical*, *24*, 102063. https://doi.org/10.1016/j.nicl.2019.102063

Bluemke, D. A., Kronmal, R. A., Lima, J. A. C., Liu, K., Olson, J., Burke, G. L., & Folsom, A. R. (2008). The relationship of left ventricular mass and geometry to incident cardiovascular events. *Journal of the American College of Cardiology*, *52*(25), 2148–2155. https://doi.org/10.1016/j.jacc.2008.09.014

Bülow, R., Ittermann, T., Dörr, M., Poesch, A., Langner, S., Völzke, H., Hosten, N., & Dewey, M. (2018). Reference ranges of left ventricular structure and function assessed by contrast-enhanced cardiac MR and changes related to ageing and hypertension in a population-based study. *European Radiology*, *28*(9), 3996–4005. https://doi.org/10.1007/s00330-018-5345-y

Cermakova, P., Muller, M., Armstrong, A. C., Religa, D., Bryan, R. N., Lima, J. A. C., & Launer, L. J. (2017). Subclinical cardiac dysfunction and brain health in midlife: CARDIA (coronary artery risk development in young adults) brain magnetic resonance imaging substudy. *Journal of the American Heart Association*, *6*(12), e006750. https://doi.org/10.1161/JAHA.117.006750

Cole, J. H., Ritchie, S. J., Bastin, M. E., Valdés Hernández, M. C., Muñoz Maniega, S., Royle, N., Corley, J., Pattie, A., Harris, S. E., Zhang, Q., Wray, N. R., Redmond, P., Marioni, R. E., Starr, J. M., Cox, S. R., Wardlaw, J. M., Sharp, D. J., & Deary, I. J. (2018). Brain age predicts mortality. *Molecular Psychiatry*, *23*(5), 1385–1392. https://doi.org/10.1038/mp.2017.62

Cuspidi, C., Meani, S., Negri, F., Giudici, V., Valerio, C., Sala, C., Zanchetti, A., & Mancia, G. (2009). Indexation of left ventricular mass to body surface area and height to allometric power of 2.7: Is the difference limited to obese hypertensives? *Journal of Human Hypertension*, *23*(11), 728–734. https://doi.org/10.1038/jhh.2009.16

Dai, D. F., Chen, T., Johnson, S. C., Szeto, H., & Rabinovitch, P. S. (2012). Cardiac aging: From molecular mechanisms to significance in human health and disease. *Antioxidants & Redox Signaling*, *16*(12), 1492–1526. https://doi.org/10.1089/ars.2011.4179

de Bruijn, R. F. A. G., Portegies, M. L. P., Leening, M. J. G., Bos, M. J., Hofman, A., van der Lugt, A., Niessen, W. J., Vernooij, M. W., Franco, O. H., Koudstaal, P. J., & Ikram, M. A. (2015). Subclinical cardiac dysfunction increases the risk of stroke and dementia: The Rotterdam study. *Neurology*, *84*(8), 833–840. https://doi.org/10.1212/WNL.0000000000001289

de Lange, A. M. G., & Cole, J. H. (2020). Commentary: Correction procedures in brain-age prediction. *NeuroImage: Clinical*, *26*, 102229. https://doi.org/10.1016/j.nicl.2020.102229

Debette, S., Seshadri, S., Beiser, A., Au, R., Himali, J. J., Palumbo, C., Wolf, P. A., & DeCarli, C. (2011). Midlife vascular risk factor exposure accelerates structural brain aging and cognitive decline. *Neurology*, *77*(5), 461–468. https://doi.org/10.1212/WNL.0b013e318227b227

Desikan, R. S., Ségonne, F., Fischl, B., Quinn, B. T., Dickerson, B. C., Blacker, D., Buckner, R. L., Dale, A. M., Maguire, R. P., Hyman, B. T., Albert, M. S., & Killiany, R. J. (2006). An automated labeling system for subdividing the human cerebral cortex on MRI scans into gyral based regions of interest. *NeuroImage*, *31*(3), 968–980. https://doi.org/10.1016/j.neuroimage.2006.01.021

Devereux, R. B., Alonso, D. R., Lutas, E. M., Gottlieb, G. J., Campo, E., Sachs, I., & Reichek, N. (1986). Echocardiographic assessment of left ventricular hypertrophy: Comparison to necropsy findings. *The American Journal of Cardiology*, *57*(6), 450–458. https://doi.org/10.1016/0002-9149(86)90771-x

Devereux, R. B., de Simone, G., Ganau, A., Koren, M. J., Mensah, G. A., & Roman, M. J. (1993). Left ventricular hypertrophy and hypertension. *Clinical and Experimental Hypertension*, *15*(6), 1025–1032. https://doi.org/10.3109/10641969309037090

Drazner, M. H., Dries, D. L., Peshock, R. M., Cooper, R. S., Klassen, C., Kazi, F., Willett, D. W., & Victor, R. G. (2005). Left ventricular hypertrophy is more prevalent in blacks than whites in the general population. *Hypertension*, *46*(1), 124–129. https://doi.org/10.1161/01.HYP.0000169972.96201.8e

Fischl, B. (2012). FreeSurfer. *Neuroimage*, *62*(2), 774–781. https://doi.org/10.1016/j.neuroimage.2012.01.021

Frenzel, S., Wittfeld, K., Bülow, R., Völzke, H., Friedrich, N., Habes, M., Felix, S. B., Dörr, M., Grabe, H. J., & Bahls, M. (2021). Cardiac hypertrophy is associated with advanced brain aging in the general population. *Journal of the American Heart Association*, *10*(17), e020994. https://doi.org/10.1161/JAHA.121.020994

Frenzel, S., Wittfeld, K., Habes, M., Klinger-König, J., Bülow, R., Völzke, H., & Grabe, H. J. (2020). A biomarker for Alzheimer's disease based on patterns of regional brain atrophy. *Frontiers in Psychiatry*, *10*. https://doi.org/10.3389/fpsyt.2019.00953

Georgakis, M. K., Synetos, A., Mihas, C., Karalexi, M. A., Tousoulis, D., Seshadri, S., & Petridou, E. T. (2017). Left ventricular hypertrophy in association with cognitive impairment: A systematic review and meta-analysis. *Hypertension Research*, *40*(7), 696–709. https://doi.org/10.1038/hr.2017.11

Griffanti, L., Zamboni, G., Khan, A., Li, L., Bonifacio, G., Sundaresan, V., Schulz, U. G., Kuker, W., Battaglini, M., Rothwell, P. M., & Jenkinson, M. (2016). BIANCA (brain intensity AbNormality classification algorithm): A new tool for automated segmentation of white matter hyperintensities. *NeuroImage*, *141*, 191–205. https://doi.org/10.1016/j.neuroimage.2016.07.018

Haidar, M. A., van Buchem, M. A., Sigurdsson, S., Gotal, J. D., Gudnason, V., Launer, L. J., & Mitchell, G. F. (2021). Wave reflection at the origin of a first-generation branch artery and target organ protection. *Hypertension*, *77*(4), 1169–1177. https://doi.org/10.1161/HYPERTENSIONAHA.120.16696

Haring, B., Omidpanah, A., Suchy-Dicey, A. M., Best, L. G., Verney, S. P., Shibata, D. K., Cole, S. A., Ali, T., Howard, B. V., Buchwald, D., & Devereux, R. B. (2017). Left ventricular mass, brain MRI and cognitive performance: Results from the strong heart study. *Hypertension*, *70*(5), 964–971. https://doi.org/10.1161/HYPERTENSIONAHA.117.09807

Harrell, F. (2015). *Regression modeling strategies: With applications to linear models, logistic and ordinal regression, and survival analysis* (2nd ed.). Springer International Publishing. https://www.springer.com/de/book/9783319194240

Hertel, J., Frenzel, S., König, J., Wittfeld, K., Fuellen, G., Holtfreter, B., Pietzner, M., Friedrich, N., Nauck, M., Völzke, H., Kocher, T., & Grabe, H. J. (2018). The informative error: A framework for the construction of individualized phenotypes. *Statistical Methods in Medical Research*, *28*(5), 1427–1438. https://doi.org/10.1177/0962280218759138

Hosten, N., Bülow, R., Völzke, H., Domin, M., Schmidt, C. O., Teumer, A., Ittermann, T., Nauck, M., Felix, S., Dörr, M., Markus, M. R. P., Völker, U., Daboul, A., Schwahn, C., Holtfreter, B., Mundt, T., Krey, K. F., Kindler, S., Mksoud, M., … Kromrey, M. L. (2022). SHIP-MR and radiology: 12 years of whole-body magnetic resonance imaging in a single center. *Healthcare*, *10*(1), 33. https://doi.org/10.3390/healthcare10010033

Johansen, M. C., Shah, A. M., Lirette, S. T., Griswold, M., Mosley, T. H., Solomon, S. D., & Gottesman, R. F. (2018). Associations of echocardiography markers and vascular brain lesions: The ARIC study. *Journal of the American Heart Association*, *7*(24), e008992. https://doi.org/10.1161/JAHA.118.008992

Kähönen-Väre, M., Brunni-Hakala, S., Lindroos, M., Pitkala, K., Strandberg, T., & Tilvis, R. (2004). Left ventricular hypertrophy and blood pressure as predictors of cognitive decline in old age. *Aging Clinical and Experimental Research*, *16*(2), 147–152. https://doi.org/10.1007/bf03324544

Kario, K. (2018). Nocturnal hypertension. *Hypertension*, *71*(6), 997–1009. https://doi.org/10.1161/HYPERTENSIONAHA.118.10971

Lakatta, E. G., & Levy, D. (2003). Arterial and cardiac aging: Major shareholders in cardiovascular disease enterprises. *Circulation*, *107*(2), 346–354. https://doi.org/10.1161/01.CIR.0000048893.62841.F7

Lang, R. M., Badano, L. P., Mor-Avi, V., Afilalo, J., Armstrong, A., Ernande, L., Flachskampf, F. A., Foster, E., Goldstein, S. A., Kuznetsova, T., Lancellotti, P., Muraru, D., Picard, M. H., Rietzschel, E. R., Rudski, L., Spencer, K. T., Tsang, W., & Voigt, J. U. (2015). Recommendations for cardiac chamber quantification by echocardiography in adults: An update from the American Society of Echocardiography and the European Association of Cardiovascular Imaging. *European Heart Journal Cardiovascular Imaging*, *16*(3), 233–270. https://doi.org/10.1093/ehjci/jev014

Lee, W. J., Jung, K. H., Ryu, Y. J., Lee, S. T., Park, K. I., Chu, K., Kim, M., Lee, S. K., & Roh, J. K. (2020). Echocardiographic index E/e' in association with cerebral white matter hyperintensity progression. *PLoS One*, *15*(7), e0236473. https://doi.org/10.1371/journal.pone.0236473

Lorell, B. H., & Carabello, B. A. (2000). Left ventricular hypertrophy. *Circulation*, *102*(4), 470–479. https://doi.org/10.1161/01.CIR.102.4.470

Mahinrad, S., Vriend, A. E., Jukema, J. W., van Heemst, D., Sattar, N., Blauw, G. J., Macfarlane, P. W., Clark, E. N., de Craen, A. J. M., & Sabayan, B. (2017). Left ventricular hypertrophy and cognitive decline in old age. *Journal of Alzheimer's Disease*, *58*(1), 275–283. https://doi.org/10.3233/JAD-161150

Markus, M. R. P., Ittermann, T., Drzyzga, C. J., Bahls, M., Schipf, S., Siewert-Markus, U., Baumeister, S. E., Schumacher, P., Ewert, R., Völzke, H., Steinhagen-Thiessen, E., Bülow, R., Schunkert, H., Vasan, R. S., Felix, S. B., & Dörr, M. (2021). Cardiac MRI shows an association of lower cardiorespiratory fitness with decreased myocardial mass and higher cardiac stiffness in the general population—The Sedentary's heart. *Progress in Cardiovascular Diseases*, *68*, 25–35. https://doi.org/10.1016/j.pcad.2021.09.003

Mitchell, G. F., van Buchem, M. A., Sigurdsson, S., Gotal, J. D., Jonsdottir, M. K., Kjartansson, Ó., Garcia, M., Aspelund, T., Harris, T. B., Gudnason, V., & Launer, L. J. (2011). Arterial stiffness, pressure and flow pulsatility and brain structure and function: The age, gene/environment susceptibility—Reykjavik study. *Brain*, *134*(11), 3398–3407. https://doi.org/10.1093/brain/awr253

Moazzami, K., Ostovaneh, M. R., Ambale Venkatesh, B., Habibi, M., Yoneyama, K., Wu, C., Liu, K., Pimenta, I., Fitzpatrick, A., Shea, S., McClelland, R. L., Heckbert, S., Gottesman, R. F., Bluemke, D. A., Hughes, T. M., & Lima, J. A. C. (2018). Left ventricular hypertrophy and remodeling and risk of cognitive impairment and dementia. *Hypertension*, *71*(3), 429–436. https://doi.org/10.1161/HYPERTENSIONAHA.117.10289

Nakanishi, K., Jin, Z., Homma, S., Elkind, M. S. V., Rundek, T., Tugcu, A., Yoshita, M., DeCarli, C., Wright, C. B., Sacco, R. L., & di Tullio, M. R. (2017). Left ventricular mass-geometry and silent cerebrovascular disease: The cardiovascular abnormalities and brain lesions (CABL) study. *American Heart Journal*, *185*, 85–92. https://doi.org/10.1016/j.ahj.2016.11.010

Papadopoulos, A., Palaiopanos, K., Protogerou, A. P., Paraskevas, G. P., Tsivgoulis, G., & Georgakis, M. K. (2020). Left ventricular hypertrophy and cerebral small vessel disease: A systematic review and meta-analysis. *Journal of Stroke*, *22*(2), 206–224. https://doi.org/10.5853/jos.2019.03335

Payabvash, S., Souza, L. C. S., Wang, Y., Schaefer, P. W., Furie, K. L., Halpern, E. F., Gonzalez, R. G., & Lev, M. H. (2011). Regional ischemic vulnerability of the brain to hypoperfusion. *Stroke*, *42*(5), 1255–1260. https://doi.org/10.1161/STROKEAHA.110.600940

Rawlings, J. O., Pantula, S. G., & Dickey, D. A. (1998). *Applied regression analysis: A research tool* (2nd ed.). Springer-Verlag. https://doi.org/10.1007/b98890

Reiter, K., Nielson, K. A., Smith, T. J., Weiss, L. R., Alfini, A. J., & Smith, J. C. (2015). Improved cardiorespiratory fitness is associated with increased cortical thickness in MCI. *Journal of the International Neuropsychological Society*, *21*(10), 757–767. https://doi.org/10.1017/S135561771500079X

Restrepo, C., Patel, S. K., Rethnam, V., Werden, E., Ramchand, J., Churilov, L., Burrell, L. M., & Brodtmann, A. (2018). Left ventricular hypertrophy and cognitive function: A systematic review. *Journal of Human Hypertension*, *32*(3), 171–179. https://doi.org/10.1038/s41371-017-0023-0

Reuter, M., Schmansky, N. J., Rosas, H. D., & Fischl, B. (2012). Within-subject template estimation for unbiased longitudinal image analysis. *NeuroImage*, *61*(4), 1402–1418. https://doi.org/10.1016/j.neuroimage.2012.02.084

Ruwhof, C., & van der Laarse, A. (2000). Mechanical stress-induced cardiac hypertrophy: Mechanisms and signal transduction pathways. *Cardiovascular Research*, *47*(1), 23–37. https://doi.org/10.1016/S0008-6363(00)00076-6

Schiller, N. B., Shah, P. M., Crawford, M., DeMaria, A., Devereux, R., Feigenbaum, H., Gutgesell, H., Reichek, N., Sahn, D., Schnittger, I., Silverman, N. H., & Tajik, A. J. (1989). Recommendations for quantitation of the left ventricle by two-dimensional echocardiography. American Society of Echocardiography Committee on standards, subcommittee on quantitation of two-dimensional echocardiograms. *Journal of the American Society of Echocardiography*, *2*(5), 358–367. https://doi.org/10.1016/s0894-7317(89)80014-8

Schwarz, C. G., Gunter, J. L., Wiste, H. J., Przybelski, S. A., Weigand, S. D., Ward, C. P., Senjem, M. L., Vemuri, P., Murray, M. E., Dickson, D. W., Parisi, J. E., Kantarci, K., Weiner, M. W., Petersen, R. C., Jack, C. R., Jr., & Alzheimer's Disease Neuroimaging Initiative. (2016). A large-scale comparison of cortical thickness and volume methods for measuring Alzheimer's disease severity. *NeuroImage: Clinical*, *11*, 802–812. https://doi.org/10.1016/j.nicl.2016.05.017

Scuteri, A., Coluccia, R., Castello, L., Nevola, E., Brancati, A. M., & Volpe, M. (2009). Left ventricular mass increase is associated with cognitive decline and dementia in the elderly independently of blood pressure. *European Heart Journal*, *30*(12), 1525–1529. https://doi.org/10.1093/eurheartj/ehp133

Shimizu, A., Sakurai, T., Mitsui, T., Miyagi, M., Nomoto, K., Kokubo, M., Bando, Y. K., Murohara, T., & Toba, K. (2014). Left ventricular diastolic dysfunction is associated with cerebral white matter lesions (leukoaraiosis) in elderly patients without ischemic heart disease and stroke. *Geriatrics & Gerontology International*, *14*(S2), 71–76. https://doi.org/10.1111/ggi.12261

Spiegelhalter, D. (2016). How old are you, really? Communicating chronic risk through 'effective age' of your body and organs. *BMC Medical Informatics and Decision Making*, *16*(1), 104. https://doi.org/10.1186/s12911-016-0342-z

Storsve, A. B., Fjell, A. M., Tamnes, C. K., Westlye, L. T., Overbye, K., Aasland, H. W., & Walhovd, K. B. (2014). Differential longitudinal changes in cortical thickness, surface area and volume across the adult life span: Regions of accelerating and decelerating change. *The Journal of Neuroscience*, *34*(25), 8488–8498. https://doi.org/10.1523/JNEUROSCI.0391-14.2014

Strait, J. B., & Lakatta, E. G. (2012). Aging-associated cardiovascular changes and their relationship to heart failure. *Heart Failure Clinics*, *8*(1), 143–164. https://doi.org/10.1016/j.hfc.2011.08.011

Tennant, P. W. G., Arnold, K. F., Ellison, G. T. H., & Gilthorpe, M. S. (2022). Analyses of 'change scores' do not estimate causal effects in observational data. *International Journal of Epidemiology*, *51*, 1604–1615. https://doi.org/10.1093/ije/dyab050

Thomas, L., Marwick, T. H., Popescu, B. A., Donal, E., & Badano, L. P. (2019). Left atrial structure and function, and left ventricular diastolic dysfunction: JACC state-of-the-art review. *Journal of the American*

College of Cardiology, *73*(15), 1961–1977. https://doi.org/10.1016/j.jacc.2019.01.059

Twisk, J. W. R. (2013). *Applied longitudinal data analysis for epidemiology: A practical guide* (2nd ed.). Cambridge University Press. https://doi.org/10.1017/CBO9781139342834

Valero-Mora, P. M. (2010). ggplot2: Elegant graphics for data analysis. *Journal of Statistical Software*, *35*, 1–3. https://doi.org/10.18637/jss.v035.b01

van Buuren, S., & Groothuis-Oudshoorn, K. (2011). Mice: Multivariate imputation by chained equations in R. *Journal of Statistical Software*, *45*, 1–67. https://doi.org/10.18637/jss.v045.i03

van der Veen, P. H., Geerlings, M. I., Visseren, F. L. J., Nathoe, H. M., Mali, W. P., van der Graaf, Y., Muller, M., & SMART Study Group. (2015). Hypertensive target organ damage and longitudinal changes in brain structure and function. *Hypertension*, *66*(6), 1152–1158. https://doi.org/10.1161/HYPERTENSIONAHA.115.06268

Vanderweele, T. J. (2015). *Explanation in causal inference: Methods for mediation and interaction*. Oxford University Press.

Völzke, H., Haring, R., Lorbeer, R., Wallaschofski, H., Reffelmann, T., Empen, K., Rettig, R., John, U., Felix, S. B., & Dörr, M. (2010). Heart valve sclerosis predicts all-cause and cardiovascular mortality. *Atherosclerosis*, *209*(2), 606–610. https://doi.org/10.1016/j.atherosclerosis.2009.10.030

Völzke, H., Schössow, J., Schmidt, C. O., Jürgens, C., Richter, A., Werner, A., Werner, N., Radke, D., Teumer, A., Ittermann, T., Schauer, B., Henck, V., Friedrich, N., Hannemann, A., Winter, T., Nauck, M., Dörr, M., Bahls, M., Felix, S. B., … Kocher, T. (2022). Cohort profile update: The study of health in Pomerania (SHIP). *International Journal of Epidemiology*, *51*, e372–e383. https://doi.org/10.1093/ije/dyac034

Wardlaw, J. M., Allerhand, M., Doubal, F. N., Valdes Hernandez, M., Morris, Z., Gow, A. J., Bastin, M., Starr, J. M., Dennis, M. S., & Deary, I. J. (2014). Vascular risk factors, large-artery atheroma, and brain white matter hyperintensities. *Neurology*, *82*(15), 1331–1338. https://doi.org/10.1212/WNL.0000000000000312

Weuve, J., Tchetgen Tchetgen, E. J., Glymour, M. M., Beck, T. L., Aggarwal, N. T., Wilson, R. S., Evans, D. A., & Mendes de Leon, C. F. (2012). Accounting for bias due to selective attrition: The example of smoking and cognitive decline. *Epidemiology*, *23*(1), 119–128. https://doi.org/10.1097/EDE.0b013e318230e861

Wolters, F. J., Zonneveld, H. I., Hofman, A., van der Lugt, A., Koudstaal, P. J., Vernooij, M. W., & Ikram, M. A. (2017). Cerebral perfusion and the risk of dementia. *Circulation*, *136*(8), 719–728. https://doi.org/10.1161/CIRCULATIONAHA.117.027448

SUPPORTING INFORMATION

Additional supporting information can be found online in the Supporting Information section at the end of this article.

How to cite this article: Frenzel, S., Bülow, R., Dörr, M., Felix, S. B., Friedrich, N., Völzke, H., Wittfeld, K., Grabe, H. J., & Bahls, M. (2024). Left ventricular hypertrophy as a risk factor for accelerated brain aging: Results from the Study of Health in Pomerania. *Human Brain Mapping*, *45*(3), e26567. https://doi.org/10.1002/hbm.26567